

A New Algorithm for Image Reconstruction for Positron Emission Tomography

Partha P. Mondal

Indian Institute of Science, Bangalore
partha@physics.iisc.ernet.in

K. Rajan

Indian Institute of Science, Bangalore
rajan@physics.iisc.ernet.in

Abstract

In Positron Emission Tomography, penalized iterative algorithms like MAP often results in over smooth reconstructions due to over penalizing nature of the assumed interacting potential. These algorithms fail to determine the density class of the estimate and hence penalize the pixels irrespective of the density class. In this work, a fuzzy logic based approach is proposed to model the prior which captures the nature of pixel-pixel interaction. Quantitative analysis shows that the proposed fuzzy rule based reconstruction algorithm is capable of producing comparable estimates when compared to MAP and MRP algorithms. The reconstructed images are sharper in nature and the presence of spatially confined minute features are well reconstructed due to the local nature of the penalizing fuzzy potential.

1. Introduction

Many of the present day applications such as diaonostic imaging modalities like positron emission tomography (PET), single photon emission computed tomography (SPECT) demand high quality images. Iterative algorithms like, maximum likelihood (ML) [18][8], maximum a-posteriori (MAP) [16][4][12][19][17][7] and median root prior (MRP) [13][14] algorithms are a few handful algorithms which are capable of generating good quality images in emission tomography (ET). In emission tomography, the stochastic algorithms like ML, MAP or MRP are far superior than their deterministic counterparts such as convolution back projection (CBP) [18][9] and weighted least squared (WLS) [5] etc. The superiority of ML, MAP, MRP is due their ability to incorporate the stochastic phenomenon emission statistics (Poissonian) and nearest neighbor interaction in the image reconstruction process.

Recently, a lot of interest is shown in the application of fuzzy techniques in image processing applications like interpolation [1], image restoration [2] etc. In the present work we have extended fuzzy concepts to PET image re-

construction modality. Fuzzy rule based potential consists of two major steps : Fuzzy Filtering and Fuzzy Smothing. Fuzzy filtering filters out the noise that builds up with increasing iteration [3], by distinguishing the intensity variation due to noise and due to image structure. Thereafter smoothing is performed for noisy pixels using neighboring pixels. These operations are performed iteratively untill the estimate converges and stabilizes.

2. Image Reconstruction Algorithms for PET

The measurements in PET , y_j , $j=1,\dots,M$ are modeled as independent Poisson random variables i.e, $y_j \sim Poisson(\sum_{i=1}^N \lambda_i p_{ij})$ for $j=1,\dots,M$, where λ_i , $i=1,\dots,N$ are the mean parameters of the emission process and p_{ij} is the probability that an annihilation in the i^{th} pixel is detected in j^{th} detector. The likelihood function i.e, the conditional probability for observing $\mathbf{Y} = \mathbf{y}$ given the emission parameter $\mathbf{\Lambda} = \lambda$ is the joint probability of the individual Poisson process. Maximum a posteriori (MAP) algorithm determines that estimate λ^{ML} , which maximizes the posterior density function $P(\lambda/y)$. Given a suitable prior $P(\lambda)$, MAP-reconstruction can be formulated as,

$$\lambda^{MAP} = \max_{\lambda \geq 0} [\log P(y/\lambda) + \log P(\lambda)] \quad (1)$$

Image field is assumed as Markov random field (MRF) [19] and by Hammerseley-Clifford theorem [6], image λ is characterized by Gibbs distribution,

$$P(\lambda) = \frac{1}{Z} e^{-\frac{1}{\beta} U(\lambda)} \quad (2)$$

where, Z is the normalizing constant for the distribution, β is the Gibbs hyper-parameter, and $U(\lambda) = \sum_i \sum_{j \in N_i} w_{ij} V(\lambda_i, \lambda_j)$ is Gibbs energy. w_{ij} is the weight of pixel $j \in N_i$ [12], N_i is the nearest neighbor set of pixel i and $V(\lambda_i, \lambda_j)$ is termed as the potential at site i due to the nearest neighbor elements $j \in N_i$.

Solution for eqn.(1) is very difficult due to the complicated nature of prior. Green [12] has proposed one step late

(OSL) approximation for an iterative update to the MAP-problem,

$$\lambda_i^{k+1} = \frac{\lambda_i^k}{\left[\sum_{j=1}^M p_{ij} + \frac{1}{\beta} \sum_{j \in N_i} \left(\frac{\partial V(\lambda_i, \lambda_j)}{\partial \lambda_i} \right)_{\lambda_i = \lambda_i^k} \right]} \times \sum_{j=1}^M \frac{y_j p_{ij}}{\sum_{i=1}^N \lambda_i^k p_{ij}} \quad (3)$$

Given OSL-algorithm (eqn.(3)), the next step is the proper modeling of the interacting potential $V(\lambda_i, \lambda_j)$ between the pixel at site i and $j \in N_i$. A large number of potentials have been suggested in the literature to produce desired image characteristics [12][19][14]. These potentials penalize the differences between the pixels irrespective of the density class in the nearest neighborhood. Hence resulting in artifacts like oversmoothing, streaking [14] etc.

3. Fuzzy Rule Based Potential Function

In this section, a fuzzy logic based expression for the potential is developed keeping in view the necessity of edge-preservation of the reconstructed images. This consists of two elementary steps : fuzzy filtering using directional derivatives and fuzzy smoothing. This idea is primarily borrowed from Ville et. al. [2]. Nevertheless the idea is expanded, generalized and adapted for image reconstruction applications in PET.

Derivative $\nabla^k(i, j)$ for pixel at (i, j) along the direction \hat{n} at k^{th} iteration is defined as,

$$\nabla^k(i, j) \hat{n} = |\lambda^k(i, j) - \lambda^k(*, *)| \hat{n}$$

where, $\lambda^k(*, *) \hat{n}$ represent the pixel along the unit directional vector \hat{n} .

For identifying edge in a particular direction, three elemental derivatives are chosen (see fig.1). For example to detect an edge in the N-S direction, the following three derivatives are used :

$$\nabla^k(i, j) \hat{W} = |\lambda^k(i, j) - \lambda^k(i, j-1)|$$

$$\nabla^k(i-1, j) \hat{W} = |\lambda^k(i-1, j) - \lambda^k(i-1, j-1)|$$

$$\nabla^k(i+1, j) \hat{W} = |\lambda^k(i+1, j) - \lambda^k(i+1, j-1)|$$

It is safe to assume that if 2 out of 3 elemental derivatives are small, the edge is absent in the neighborhood. This is termed a 2:3 rule. To compute the value that expresses the degree to which the fuzzy derivative in a certain direction is small, we make use of fuzzy set **small**. Based on this observation, the values of the fuzzy derivatives $\nabla_F^k(i, j) \hat{n}$

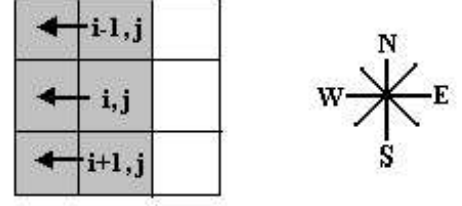


Figure 1. 3×3 neighborhood of a central pixel (i, j) , showing the directional derivative along \hat{W} .

for all the directions i.e. $\{\hat{W}, \hat{N}, \hat{S}, \hat{N}\hat{W}, \hat{S}\hat{W}, \hat{S}\hat{E}, \hat{N}\hat{E}\}$ are calculated. For example, for $\hat{n} = \hat{W}$ the value of the fuzzy derivative is defined as follows :

If

$$\begin{cases} \nabla^k(i, j) \text{ and } \nabla^k(i-1, j) \text{ are small or} \\ \nabla^k(i, j) \text{ and } \nabla^k(i+1, j) \text{ are small or} \\ \nabla^k(i-1, j) \text{ and } \nabla^k(i+1, j) \text{ are small} \end{cases}$$

Then, $\nabla_F^k(i, j) \hat{W}$ is **small**

$$\text{Else, } \nabla_F^k(i, j) \hat{W} \text{ is large} \quad (4)$$

To compute the value that expresses the degree to which the fuzzy derivative is small, we make use of fuzzy set **small**. Fuzzy sets are best represented by membership function. Membership function μ of a fuzzy set X maps the elements of X into a binary value $[0, 1]$. Membership function at site (i, j) in the direction \hat{E} at k^{th} iterations for the property **small** is defined as,

$$\mu^k(i, j) \hat{E} = \begin{cases} 0 & \text{if } \nabla_M^k(i, j) \geq \nabla^k(i, j) \\ 1, & \text{otherwise.} \end{cases} \quad (5)$$

where,

$$\nabla_M^k(i, j) \hat{E} = \text{mean}\{\nabla^k(i-1, j), \nabla^k(i, j), \nabla^k(i+1, j)\}$$

A value of 0 indicates the absence of edge while 1 indicates the presence of edge. The set **small** corresponds to 0 and **large** corresponds to 1. Similarly, along all the directions viz. $\{\hat{W}, \hat{N}, \hat{S}, \hat{N}\hat{W}, \hat{S}\hat{W}, \hat{S}\hat{E}, \hat{N}\hat{E}\}$ the membership functions are defined.

After edge detection the next step is the penalization of the noisy pixels by proper feedback of the correction value. Only those pixels for which edges are not detected in the nearest neighborhood are subjected to penalization, else they remain unaltered. The following rule is used for penalization :

If $\nabla_F^k(i, j) \hat{n}$ is **small**, Then $\Delta^k(i, j) \hat{n} = \nabla^k(i, j) \hat{n}$.

$$\text{Else, } \Delta^k(i, j) \hat{n} = 0 \quad (6)$$

where, $\Delta^k(i, j)\hat{n}$ is the feedback at site (i, j) due to the pixel in the direction \hat{n} at k^{th} iteration. Eight such rules are used to get the contribution from all the eight direction. There are 8 such rules for each of the 8 directions. Hence, the total correction term $\Delta_T^k(i, j)$ for pixel at (i, j) considering all the directions at k^{th} iteration is given by,

$$\Delta_T^k(i, j) = \frac{1}{8} \sum_{\hat{n}} \Delta^k(i, j)\hat{n} \quad (7)$$

Each direction contributes to the final correction term Δ_T^k for pixel at (i, j) . Replacing the error term $\sum_{j \in N_i} \left(\frac{\partial V(\lambda_i, \lambda_j)}{\partial \lambda_i} \right)_{\lambda_i = \lambda_i^k}$ in eqn.(3) by $\Delta_T^k(i') = \Delta_T^k(i, j)$, the OSL-algorithm modifies to,

$$\lambda_{i'}^{k+1} = \frac{\lambda_{i'}^k}{\left[\sum_{j=1}^M p_{i'j} + \frac{1}{\beta} \Delta_T^k(i') \right]} \sum_{j=1}^M \frac{y_j p_{i'j}}{\sum_{o=1}^N \lambda_o^k p_{oj}} \quad (8)$$

where, coordinates (i, j) is denoted by a single coordinate $\{i' = (i - 1) * \sqrt{N} + j\}$. In the iterative image reconstruction procedure, the final correction term is fed back to update the pixel after each iteration. The iterations are continued until acceptable convergence is obtained.

The fuzzy rules explained in the previous subsections 3.1, 3.2 and 3.3 are for the neighborhood window of size 3×3 . In this subsection the fuzzy rules are defined for 5×5 neighborhood window. In the case of 3×3 window the fuzzy directional derivative is calculated using 3 elemental derivatives per direction. The sensitivity of edge detection depends upon the number of derivatives used for edge detection. To study the effect of window size on the reconstructed image, five elemental derivatives per direction are used. For example, the elemental derivatives used for edge detection in SW direction are $\nabla^k(i, j)$, $\nabla^k(i - 1, j - 1)$, $\nabla^k(i + 1, j + 1)$, $\nabla^k(i - 2, j - 2)$ and $\nabla^k(i + 2, j + 2)$. Similarly, for all the directions 5 elemental derivatives are chosen for edge detection and 3:5 rule is used for edge detection. The membership function will have the same form except that for 5×5 window, the mean $\nabla_M^k(i, j)\hat{n}$ is taken over all the 5 elemental derivatives. The rest of the method is similar to that for 3×3 window.

4. Simulated Experimental Results

Implementation of the proposed algorithm is performed on a simulated PET system. The general description of PET system is given below.

The PET system consists of a ring detector with 64 detectors and the object space is decomposed into 64×64 square pixels. For simplicity, we assumed that i.e., $p_{ij} = \frac{\theta_{ij}}{\pi}$ [18].

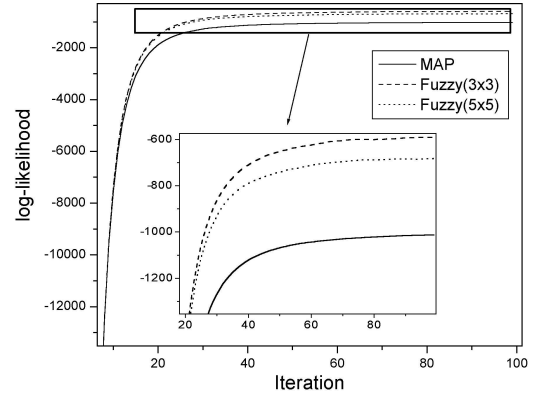


Figure 2. Log-likelihood values for MAP and proposed fuzzy algorithm with 3×3 and 5×5 window.

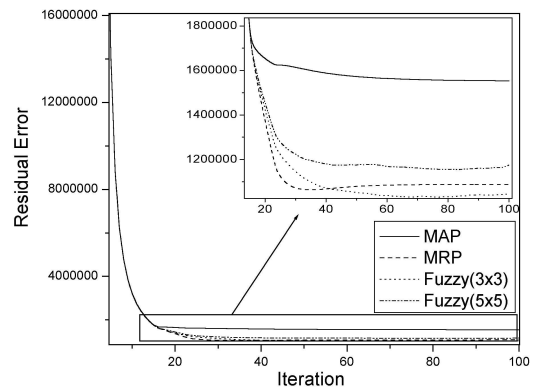


Figure 3. Residual Error plot for MAP and proposed fuzzy algorithm with 3×3 and 5×5 window.

Before the reconstruction begins, the probability matrix $\mathbf{P} = [p_{ij}]$, $i = 1, \dots, N$ and $j = 1, \dots, M$ is computed and stored. For simulating measurement data, a Monte Carlo procedure is used [18][11]. We have used a source image with 100,000 counts.

All the evaluation tests defined in this section are carried out on the proposed fuzzy algorithm with 3×3 and 5×5 neighborhood window. The results are also compared with MAP reconstruction algorithm. MAP with potential $V = (\lambda_i - \lambda_j)^2$ and $\beta = 2.5 \times 10^4$ is used in this study. This choice of β is considered because it gives the best MAP estimate. The performances of the proposed new algorithm are evaluated using three different image-based quantitative criteria as given below :

Since MAP, MRP and the proposed algorithms compute the estimate of the emission densities iteratively, hence log-likelihood function is an appropriate qualitative measure. For an estimate λ^k , the log-likelihood function $l(\lambda^k)$ at k^{th}

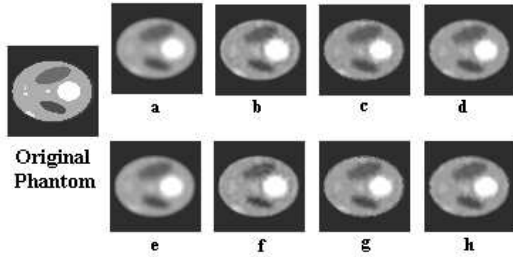


Figure 4. First row shows reconstruction after 50 iterations for (a) MAP, (b) MRP, (c) proposed algorithm. Second row shows reconstruction after 100 iterations for (d) MAP, (e) MRP, (f) proposed algorithm.

iteration is defined as,

$$l(\lambda^k) = \sum_{j=1}^M [-\phi_j^k + y_j \log \phi_j^k - \log(y_j!)] \quad (9)$$

where, $\phi_j^k = \sum_{i=1}^N \lambda_i^k P_{ij}$ is the pseudo-projection in the tube j .

The log-likelihood values of the reconstructed images obtained using MAP and proposed algorithm for both 3×3 and 5×5 are plotted against the iterations in fig.2. It is clearly evident that log-likelihood for the proposed algorithm converges faster compared to MAP-algorithm.

The second evaluation test is the residual error. This measures the deviation of the generated pseudo-projections ϕ_j^k of the reconstructed image from the observed projection data y_j . Residual error $\rho(\lambda^k)$ at k^{th} -iteration is given by,

$$\rho(\lambda^k) = \sum_{j=1}^M (y_j - \phi_j^k)^2 \quad (10)$$

In fig.3, the residual errors of the reconstructed images for the proposed algorithm with 3×3 and 5×5 window along with MAP and MRP algorithms are shown. From these plots it is clear that proposed algorithm has residual error comparable to MRP and better than MAP.

In fig.4, first and second rows show the reconstructed images using MAP, MRP, proposed algorithm for 3×3 and 5×5 after 50 and 100 iterations respectively. For visual comparison, original test image is also shown. Images reconstructed using the proposed algorithm are more appealing and rich in edges compared to MAP and MRP.

Furthermore, to quantify the reconstructed images, a small edge part of the Shepp-Logan phantom is enlarged. Fig.5 shows an enlarged portion of the reconstructions using MAP, MRP, proposed algorithm for 3×3 and 5×5 neighborhood window. For comparison, a part of original Shepp-Logan phantom is also shown in fig.5. Reconstructed im-

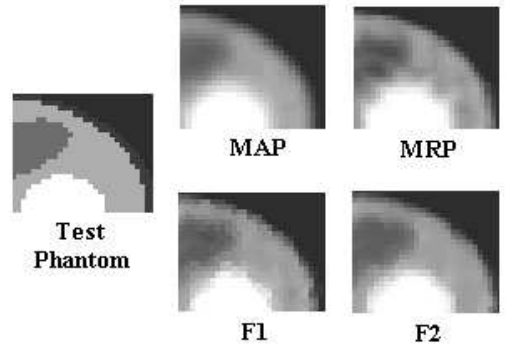


Figure 5. Enlarged part of the reconstructed images after 100 iterations.

ages using the proposed algorithm compares favorably with MAP and MRP reconstructed images.

5. Conclusions

In this paper, we have presented a new approach for edge preserving reconstructed of the emission densities in PET. This is based on the application of fuzzy rule based techniques to model the potential (which accounts for the nearest neighbor interaction) in image reconstruction problem. Two basic steps are performed namely fuzzy filtering and fuzzy smoothing. This dual operation is continued iteratively until accepted convergence is obtained. Experimental studies on a computer simulated PET system reveals that the proposed algorithm competes favorably with the existing reconstruction algorithms like MAP and MRP. Visual representation of the reconstructed planes using proposed algorithms are more appealing compared to MAP and MRP reconstructed planes. The results are very encouraging.

References

- [1] D. Van De Ville, W. Philips, and I. Lemahieu, Fuzzy Techniques in Image Processing. New York: Springer-Verlag, 2000, vol. 52, Studies in Fuzziness and Soft Computing, ch. Fuzzy-based motion detection and its application to de-interlacing, pp. 337369.
- [2] D. V. Ville, M. Nachtegaal, D. V. Weken, E. E. Kerre, W. Philips and I. Lemahieu, "Noise Reduction by Fuzzy Image Filtering", IEEE Trans. Fuzzy Sys., Vol. 11, NO. 4, Aug. 2003
- [3] E. Veclerov and J. Llacer, "Stopping rule for MLE algorithm based on statistical hypothesis testing", IEEE Trans. on Med. Img., MI-6, pp. 313-319, 1987.

- [4] E. Levitan and G.T. Herman. "A maximum a posteriori probability expectation maximization algorithm for image reconstruction in emission tomography", *IEEE Trans. on Medical Imaging* ., MI-6(3) : pp. 185-192, 1987.
- [5] J. A. Fessler, "Penalized weighted least-squares image reconstruction for positron emission tomography", *IEEE Trans. Med. Img.*, Vol.13, No.2, pp.290-300, June, 1994.
- [6] J. Besag, "Spatial interaction and the statistical analysis of lattice systems", *Jl. of Royal Stat. Soc. B*, Vol.36, pp. 192-236, 1974.
- [7] J. Nuyts, D. Bequ, P. Dupont, and L. Mortelmans, "A Concave Prior Penalizing Relative Differences for Maximum-a-Posteriori Reconstruction in Emission Tomography", *IEEE Trans. on Nuclear Science*, Vol. 49, No. 1, pp.56-60, Feb. 2002.
- [8] L.A. Shepp and Y. Vardi., "Maximum likelihood estimation for emission tomography", *IEEE Trans. on Medical Imaging* ., MI-1: pp. 113-121, 1982.
- [9] L.A. Shepp and B. F. Logan, "The Fourier Reconstruction of a Head Section", *IEEE Trans. Nucl. Img.*, NS-21, pp.21-43, 1974.
- [10] L. Kaufmann, "Implementing and accelerating the EM-algorithm for positron emission tomography", *IEEE Trans. Med. Img.*, Vol. MI-6, pp.37-51, Mar. 1987.
- [11] N. Rajeevan, K. Rajgopal and G. Krishna. "Vector-Extrapolated fast maximum likelihood estimation algorithms for emission tomography", *IEEE Trans. on Med. Img.*, Vol. 11, No.1, March 1992.
- [12] P.J. Green, "Bayesian reconstruction from emission tomography data using a modified EM algorithm", *IEEE Trans. on Med. Img.*, vol.9, No.1, March, 1990.
- [13] S. Alenius and U. Ruotsalainen, "Using Local Median as the Location of Prior Distribution in Iterative Emission Tomography Reconstruction", *IEEE Tran. Nucl. Sci.*, Vol.45, No.6, Dec. 1998.
- [14] S. Alenius and U. Ruotsalainen, "Generalization of Median Root Prior Reconstruction", *IEEE Trans. Med. Img.*, Vol.21, No.11, Nov., 2002.
- [15] S. Geman and D.Geman, "Stochastic relaxation, Gibbs distribution and the Bayesian restoration of images", *IEEE Trans. Pattern Anal. Machine Intell.*, vol. PAMI-6, pp. 721-741, Nov., 1984.
- [16] T. Hebert and R. Leahy, "A generalized EM algorithm for 3-D Bayesian reconstruction from Poisson data using Gibbs priors", *IEEE Trans. on Medical Imaging*., MI-8(2) : pp. 194-202, 1989.
- [17] T. Hebert and R. Leahy, "Statistic based MAP image reconstruction from Poisson data using Gibbs Proiors", *IEEE Trans. on Sig. Proc.*, vol. 40, No.2, pp.2290-2303, Sept. 1992.
- [18] Y. Vardi, L. A. Shepp, and L. Kaufmann, "A statistical model for positron emission tomography", *J. Amer. Stat. Assoc.*, vol. 80, pp. 8-37, 1985.
- [19] Z. Zhou, R. M. Leahy and J. Qi, "Approximate maximum likelihood hyperparameter estimation for Gibbs prior", *IEEE Trans. on Img. proc.*, Vol.6, No.6, pp.844-861, June, 1997.